

Article type : Article

Enhancement in electrical and magnetodielectric properties of Ca- and Ba-doped BiFeO₃ polycrystalline ceramics

Balakrishnan Ramachandran^{1,2,*}, Ambesh Dixit^{3,4,#}, Ratna Naik³, and M.S. Ramachandra Rao¹

¹Nano Functional Materials Technology Centre and Department of Physics, Indian Institute of Technology Madras, Chennai, 600036, Tamil Nadu, India.

²Department of Physics, National Dong Hwa University, Hualien 97401, Taiwan.

³Department of Physics and Astronomy, Wayne State University, Detroit, Michigan, 48201, USA.

⁴Department of Physics and Center for Solar Energy, Indian Institute of Technology Jodhpur, Jodhpur 342011, Rajasthan, India

Correspondence: *ramskovil@gmail.com (BR) and #ambesh@iitj.ac.in (AD)

Abstract

We carried out a comparative study on the electrical and magnetodielectric properties of polycrystalline BiFeO₃, Bi_{0.9}Ca_{0.1}FeO_{2.95}, Bi_{0.9}Ba_{0.05}Ca_{0.05}FeO_{2.95}, and Bi_{0.9}Ba_{0.1}FeO_{2.95}

This is the author manuscript accepted for publication and has undergone full peer review but has not been through the copyediting, typesetting, pagination and proofreading process, which may lead to differences between this version and the [Version of Record](#). Please cite this article as [doi: 10.1111/jace.15258](https://doi.org/10.1111/jace.15258)

ceramics. The two dielectric anomalies, near 25 K and 281 K, are observed for BiFeO₃. Interestingly, the anomaly near 25 K shifts towards a higher temperature above 60 K with Ca and/or Ba doping, attributed to the doping induced chemical pressure. In addition, the room temperature switchable magnetodielectric effect is witnessed for the doped BiFeO₃ compounds, due to the quadratic magnetoelectric coupling. This indicates the improved magnetoelectric coupling in BiFeO₃ with the Ca and Ba doping. This is essentially due to the enhanced magnetic ordering and reduced leakage current in BiFeO₃ after the doping.

KEYWORDS: multiferroics, oxides, dielectric materials/properties, electrical properties

1. INTRODUCTION

Bismuth ferrite (BiFeO₃) is one of the most widely studied multiferroic materials in the literature due to the coexistence of ferroelectric and magnetic ordering at room temperature (RT) and hence it is a potential material for functional electronic devices.¹⁻⁶ This material is ferroelectric below the Curie temperature, $T_C = 1100$ K and exhibits antiferromagnetic ordering below the Néel temperature, $T_N = 643$ K.⁶ In fact, multiferroic materials have gained enormous attention due to their potential in microelectronic and spintronic applications,^{7,8} and the possibility of controlling magnetization (M) by electric fields or polarization (P) by magnetic fields.⁹⁻¹¹ Particularly, the magnetoelectric (ME) coupling is one of the most important material parameters of multiferroics,¹²⁻¹⁵ and is measured directly using a dynamic ME effect.^{9,10} While magnetodielectric (MD) effect has been used as an indirect method to probe ME coupling in multiferroic systems.¹⁵⁻¹⁸

The intrinsic dielectric properties such as polarization and dielectric permittivity of BiFeO₃ near RT are usually hampered by its large electrical conductivity. In this respect, the frequency-dependent dielectric properties of bulk BiFeO₃ over the temperature range of 10–300 K were studied by Kamba *et al.*¹⁹ They attributed an anomaly near 250 K to the Maxwell-Wagner (MW) contribution for permittivity as a result of a relaxation arising at the interfaces between grains and grain boundaries.^{19,20} At low frequencies or at high temperatures, colossal dielectric constants are also reported due to an increased electrical conductivity, which leading to the MW effects.²¹⁻²³ The temperature at which

the MW relaxation begins to dominate the dielectric response depends on the sample conductivity; this could be as low as 200 K for some samples.¹⁹

Recently, we have investigated the effects of oxygen non-stoichiometry on the structural and dielectric properties of bulk BiFeO₃.²⁴ We found that the coupling among spin, lattice, and charge degrees of freedom persists down to low temperatures (<30 K) and furthermore these properties depend on the degree of oxygen non-stoichiometry.²⁴ One of the primary mechanisms that produce ME coupling in BiFeO₃ is the interactions between spin waves (magnons) and polarization waves (optical phonons)^{25,26}, which results in low-frequency magneto-optical resonances in the dielectric susceptibility²⁶. These so-called electromagnetic excitations²⁶ (electromagnon – magnon with electric dipole activity) could be related to the dielectric anomaly below 100 K in the undoped and Ca-doped BiFeO₃ compounds.^{24,27} We also observed the improved MD effect in polycrystalline Bi_{0.9}Ca_{0.1}FeO_{2.95}, presumably due to the nonlinear ME coupling.²⁷

In a recent study, Ramachandran *et al.*²⁸ showed that both phonon (acoustic and optical) and magnon transport heat in the BiFeO₃-based samples using the thermal conductivity and magneto-thermal conductivity measurements. Remarkably, the dip in thermal conductivity near the low-*T* dielectric anomaly was seen for the undoped and Ca-doped BiFeO₃ ceramics,^{24,27,28} presumably due to the phonon-magnon coupling.²⁸ Notably, this study revealed that the Ca doping enhances the optical phonon thermal transport, particularly optical phonon-magnon resonant contribution. These findings are essentially attributed to the chemical pressure induced by Ca that leads to an enhanced magnetic ordering and the softening of phonon modes. Very recently, Caspers *et al.*²⁹ also observed a dip feature near 50 K in the spectral weight of the spin cycloid resonance (SCR) peaks in stoichiometric polycrystalline BiFeO₃, which ascribed to the phonon-magnon coupling. Hence, in the present work, we conducted a study to compare Ca- and Ba-doped BiFeO₃ ceramic samples with BiFeO₃ using the dielectric, magnetodielectric, and leakage current measurements. This study has been done to optimize the materials properties of BiFeO₃-based samples for the electroceramic devices.³⁰⁻³²

2. EXPERIMENTAL PROCEDURE

Synthesis of polycrystalline BiFeO₃, Bi_{0.9}Ca_{0.1}FeO_{2.95}, Bi_{0.9}Ba_{0.05}Ca_{0.05}FeO_{2.95}, and Bi_{0.9}Ba_{0.1}FeO_{2.95} samples was carried out using a sol-gel approach, described

elsewhere.^{6,33} The obtained powder samples were sintered in air at 1123 K for 6 hours. We noticed that $\text{Bi}_{0.9}\text{Ca}_{0.1}\text{FeO}_{2.95}$ samples have a slightly lower relative density (~88%) than BiFeO_3 (~90%). However, Ba doping led to an improved densification (~92%).³¹ Here, we have restricted the doping concentration of Ca and Ba at $x = 0.1$, because the Ca doping in BiFeO_3 ($\text{Bi}_{1-x}\text{Ca}_x\text{FeO}_3$) results in the ferroelectric-paraelectric transition at $x \sim 0.125$.³⁴ In addition, the doping of alkali-earth-metals in BiFeO_3 leads to the structural transition at higher contents ($x \geq 0.1$). Indeed, all studied samples are crystallized in the rhombohedral crystal symmetry with $R3c$ space group,³³ which is essential to seize ME coupling in the doped BiFeO_3 .

Notably, the doping of Ca and Ba in the BiFeO_3 lattice has resulted in the reduction in unit cell parameters.³³ For instance, the unit cell volume of the doped samples is decreased to $< 370 \text{ \AA}^3$ from the value of about 374.4 \AA^3 for BiFeO_3 . In addition, the Fe1-O-Fe2 bond length of the doped BiFeO_3 samples is also decreased slightly as compared to BiFeO_3 . Besides, we also confirmed the presence of oxygen vacancy and the valence state of Fe (3+) in the doped BiFeO_3 samples using X-ray photoelectron spectroscopic studies. As a result of these structural changes by the doping, the magnetic properties of the doped samples are enhanced considerably as compared to BiFeO_3 .³³ On the other hand, the ferroelectric properties of the Ba-doped BiFeO_3 samples are improved than that of BiFeO_3 . i.e., the maximum polarization of $\text{Bi}_{0.9}\text{Ba}_{0.1}\text{FeO}_{2.95}$ at an applied voltage of 4 kV is about $P_{max} = 1.2 \text{ \mu C/cm}^2$, which is twice higher than that of BiFeO_3 . Thus, the coupling between different order parameters such as spin, charge, and lattice in the doped BiFeO_3 (especially Ca-doped) compounds is enhanced noticeably.^{24,27,28}

In the current work, we present a comparative study on the electrical and magnetodielectric properties of BiFeO_3 -based materials with Ca and/or Ba doping at the Bi-site. The temperature-dependent dielectric constant (ϵ_r) and dielectric loss ($\tan\delta$) of undoped and doped BiFeO_3 ceramic samples are measured in the temperature range of 10–350 K, using a precision LCR meter (Agilent 4284A), coupled with a physical property measurement system (PPMS, Quantum design) for controlling both temperature and magnetic field, as per needs. The dielectric measurements are performed with an applied voltage of 1 V at a frequency of 30 kHz. We also carried out the magnetodielectric and leakage current (J - V) measurements on these samples at RT using

the LCR meter and Radiant ferroelectric loop tracer, respectively. Here, it is important to note that the stability of the capacitance measurements using the Agilent 4284A LCR meter is about 0.01%. Furthermore, the precision values of the capacitance and leakage current measurements are about 0.01 fF and 10 pA, respectively.

3. RESULTS AND DISCUSSION

The temperature-dependent dielectric constant (ϵ_r) and dielectric loss ($\tan\delta$) of the undoped and doped BiFeO₃ samples measured at 30 kHz are presented in Figs. 1a and 1b, respectively. We found the enhanced dielectric constant over the entire temperature range upon the doping. The dielectric loss of the Ba-doped BiFeO₃ is slightly smaller than BiFeO₃ near RT, while the dielectric loss increases for both Ca-doped and Ba-Ca co-doped samples (Fig. 1b). However, above 200 K, the observed large dielectric constant for the undoped, Ca-doped, and Ba-Ca co-doped BiFeO₃ samples suggests the development of an MW effect, and is associated with the increased electrical conductivity near RT.^{19,20} However, the Ba-doped BiFeO₃ seems to display entirely intrinsic behavior over the investigated temperature range of 10–350 K.

The two dielectric anomalies near 25 K and 281 K are clearly visible for BiFeO₃, Fig. 1b. The low- T anomaly is attributed to a magnetic transition with magnetoelectric coupling and magnetic glassy behavior.^{24,27} Interestingly, the anomaly near 25 K showed a noticeable shift towards higher temperature >60 K and broadened considerably with the doping (inset, Fig. 1b). The values of peak temperatures of the low- T dielectric anomaly are about 25 K, 68 K, 98 K, and 109 K for the undoped, Ca-, Ba-Ca-, and Ba-doped BiFeO₃ samples, respectively. At lower temperatures <100 K, the frequency-dependent dielectric constant of the Ca-doped BiFeO₃ samples can be fitted to a Vogel-Fulcher equation,²⁷ implying the glassy behavior. This is similar to the conventional relaxor ferroelectric behavior. While the undoped and Ba-doped BiFeO₃ samples follow an Arrhenius relation, signifying the superparaelectric behavior for these samples.^{24,27} Importantly, it is noted that the dielectric relaxation time of the Ca-doped BiFeO₃ samples is in order of 10^{-8} s in the low- T region, which is higher than that of the undoped and Ba-doped samples ($\leq 10^{-10}$ s). On the other hand, the high- T dielectric

anomaly above 250 K is broadened for the Ca-doped and Ba-Ca co-doped samples as compared to that of BiFeO₃. Here, the observed high-*T* anomaly is due to the MW relaxation at the interfaces between grains and grain boundaries.¹⁹ However, the high-*T* anomaly has vanished for the Ba-doped BiFeO₃, which is clearly evident in Fig. 1b. The absence of this feature can be associated with the disappearance of antiferromagnetic to spin glass transition in the Ba-doped BiFeO₃,³³ which confirms a link between the development of magnetic glassy behavior and the high-*T* dielectric anomaly.

To probe the spin-charge coupling in the undoped and doped BiFeO₃ samples, we studied the RT MD effect by measuring the magnetic field (*H*) modulated dielectric constant (ϵ_r) up to 80 kOe. The relative change in dielectric constant ($\Delta\epsilon/\epsilon = \Delta\epsilon(H)/\epsilon(0)$) is computed (illustrated in Fig. 2) using the relation:

$$\frac{\Delta\epsilon(H)}{\epsilon(0)} = \frac{\epsilon(H) - \epsilon(0)}{\epsilon(0)}, \quad (1)$$

where $\epsilon(H)$ and $\epsilon(0)$ are the dielectric constants with and without an applied magnetic field. We noticed that the $\Delta\epsilon/\epsilon$ value at a magnetic field of 80 kOe is about 1.12%, 0.22%, 0.15%, and 0.03% for BiFeO₃, Bi_{0.9}Ca_{0.1}FeO_{2.95}, Bi_{0.9}Ba_{0.05}Ca_{0.05}FeO_{2.95}, and Bi_{0.9}Ba_{0.1}FeO_{2.95}, respectively. The MD effect in BiFeO₃ shows a linear increase in dielectric constant with increasing *H* (Fig 2a) and has higher $\Delta\epsilon/\epsilon$ values than the doped samples. This behavior of BiFeO₃ is most likely due to an improper MD effect such as the MW effect and magnetoresistance;¹⁹ but not due to the coupling between the spontaneous polarization and magnetization. This is due to fact that the linear ME effect should not occur in BiFeO₃ due to its cycloidal *G*-type antiferromagnetic structure.^{19,35} Actually, the undoing of this magnetic ordering can only happen at higher fields >160 kOe.^{35,36} It should also be noted here that the linear shift in dielectric constant at certain fields reflecting some background effect and is not the intrinsic property of BiFeO₃.

On the other hand, MD effect is changed drastically with the Ca and Ba doping in the Bi-sites of BiFeO₃ (Fig 2b). Notably, these materials display a distorted butterfly-like loop behavior, contrary to the linear behavior of BiFeO₃ (Fig. 2a). This finding implies that the MD effect in the doped BiFeO₃ compounds has improved considerably when compared to BiFeO₃ in which the intrinsic ME effect is non-traceable (or trivial). In fact,

a quadratic-type magnetodielectric coupling is expected for these ME multiferroic systems, i.e. the shift in dielectric constant proportional to the square of H in the magnetically ordered phase. Hence, the observed nonlinear MD effects in the doped BiFeO₃ materials can be ascribed to a bi-quadratic term in the Ginzburg-Landau free energy, P^2M^2 ,²⁷ which always allowed by the symmetry.

In general, the relative change in dielectric constant ($\Delta\varepsilon/\varepsilon$) below T_N is proportional to the magnetic order parameter, since the magnetization (M) is proportional to magnetic field (H), which can be written as

$$\frac{\Delta\varepsilon(H)}{\varepsilon(0)} = \gamma H^m. \quad (2)$$

Here, the sign of $\Delta\varepsilon/\varepsilon$ depends on the sign of the ME interaction constant $\gamma(T)$ which can be either positive or negative depending on the nature of ME coupling, and m is the power factor. Importantly, the absolute value of $\Delta\varepsilon/\varepsilon$ will increase as the square of the spontaneous magnetization at a given temperature. However, it is hard to confirm this experimentally, mainly due to the difficulties in estimating the ε values for the paramagnetic phase below T_N . In fact, the contribution of the improper MD effect to the doped BiFeO₃ samples cannot be ignored entirely.¹⁹ Yet, we have tried a nonlinear fit to the data of $\Delta\varepsilon/\varepsilon$ versus H for the doped BiFeO₃ samples using the Eq. 2, which is illustrated by the solid lines in Fig. 3. However, at higher magnetic fields (>44 kOe), the $\Delta\varepsilon/\varepsilon$ value tends to saturate for the doped BiFeO₃ samples (Fig. 3), presumably due to the tendency of saturation in magnetization at higher H .^{27,33} Notably, the fitting reveals that the ME interaction constant, γ (in order of ppb) is higher for the Bi_{0.9}Ca_{0.1}FeO_{2.95} sample than the Ba-doped samples, which is due to the increase in the magnetic susceptibility with the Ca doping.³³ While the value of power factor (m) is estimated to be higher (~1.3) for the Bi_{0.9}Ba_{0.05}Ca_{0.05}FeO_{2.95} as compared to other doped samples (~1.2).

To further clarify these observations, we have plotted the relative change in dielectric constant ($\Delta\varepsilon/\varepsilon$) versus magnetization (M), as shown in Fig. 3b, using the first-quarter M - H data for the doped samples that presented in our earlier report.³³ From this graph, it is clear that the $\Delta\varepsilon/\varepsilon$ value of the doped BiFeO₃ samples increases with increasing M (or H), presumably due to the proper ME effect. Among these doped samples, the Ba-Ca co-

doped sample displays a better MD behavior, as it showed a gradual variation in $\Delta\epsilon/\epsilon$ with M over the wide range of magnetic fields, without any saturation effects at higher fields (unlike the sample $\text{Bi}_{0.9}\text{Ca}_{0.1}\text{FeO}_{2.95}$). Most importantly, the observed nonlinear and switchable MD effect in the Ca-doped BiFeO_3 ceramic materials can be explained by the enhancement of weak ferromagnetic moments,³³ due to the energy gain of the Dzyaloshinskii-Moriya (DM) interaction under an external magnetic field that tend to align with H .^{37,38} That's why, the Ca-doped samples showed a better MD effect than the Ba-doped BiFeO_3 , which is mainly due to the improvement in the magnetic properties of BiFeO_3 with Ca content.³³ This means that the applied H can increase the polarization in the doped BiFeO_3 samples via the DM interaction and hence the improved ME properties for the doped samples is witnessed here.

Besides, it is obvious that the presented data, $\Delta\epsilon/\epsilon$ versus H or M (see Figs. 2-3) of the doped BiFeO_3 samples display a dynamic behavior; however, the experimental error in the dielectric measurements is expected to be a static one. Hence, we propose that the observed MD effect in the doped samples is an intrinsic material behavior. Whereas BiFeO_3 shows a peculiar behavior (inset of Fig. 3b), e.g., the plateau features at the certain fields, likely due to the improper ME effects.¹⁹ For example, the $\Delta\epsilon/\epsilon$ value increases continuously with increasing or decreasing magnetic field (see Fig. 2a), which is possibly due to the continuous relaxing of ferroic domains in BiFeO_3 while varying the field (i.e., its ferroic domains relatively insensitive to the applied field). This means that this sample takes unusually long time to come to a static value for a given field. Thus, the MD effect in BiFeO_3 is completely different from that in the doped samples.

Furthermore, in an earlier work,³³ Ramachandran *et al.* showed that both remnant magnetization (M_r) and coercive field (H_C) improved substantially for the Ca-doped BiFeO_3 samples as compared to BiFeO_3 . In addition, the antiferromagnetic transition temperature (T_N) is also increased to 645 K with Ca doping ($\text{Bi}_{0.9}\text{Ca}_{0.1}\text{FeO}_{2.95}$ and $\text{Bi}_{0.9}\text{Ba}_{0.05}\text{Ca}_{0.05}\text{FeO}_{2.95}$) from 643 K of BiFeO_3 . This is mainly credited to the induced chemical pressure by the Ca doping in BiFeO_3 .³³ Besides, the value of magnetic susceptibility of the Ca-doped samples showed the sharp increase with lowering temperature near T_N , which is attributed to a sharp rise in the paramagnetic susceptibility at around T_N . This is essentially due to the antisymmetric spin coupling via an anisotropic

superexchange interaction.³⁹ As a result, a weak ferromagnetic ordering is being induced in the Ca-doped BiFeO₃ samples,³³ which eventually leads to the enhanced ME coupling in BiFeO₃ with Ca doping (see Figs. 2-3).^{27,28} Besides, we also attribute the reduced leakage current behavior of these doped samples for showing the improved MD effect, which is discussed in the following.

Figure 4 illustrates the electric voltage dependence of leakage current density (J - V) for the undoped and doped BiFeO₃ samples at RT. The samples in disc form with about 1 mm thickness are used for this study. Under the same testing voltage, the doped BiFeO₃ samples have a lower leakage current density than BiFeO₃. At the applied voltage of 4 kV, the leakage current density of BiFeO₃, Bi_{0.9}Ca_{0.1}FeO_{2.95}, Bi_{0.9}Ba_{0.05}Ca_{0.05}FeO_{2.95}, and Bi_{0.9}Ba_{0.1}FeO_{2.95} samples are about 8.5×10^{-4} A/cm², 1.7×10^{-4} A/cm², 5.8×10^{-5} A/cm², and 5.6×10^{-5} A/cm², respectively. The Ba-doped BiFeO₃ showed a lowest leakage current density among the examined samples, analogous to its dielectric loss value (Fig. 1b). In particular, its value is estimated to be about 15 times lower than BiFeO₃. In addition, the Ba-Ca co-doped sample showed a similar leakage current density to that of Bi_{0.9}Ba_{0.1}FeO_{2.95}.

The inset of Fig. 4 shows logarithmic plots of the current density (J) versus the electric voltage (V) for the studied samples. The slope of this curve in the low voltage range (or near the origin) is close to ~1, consistent with the Ohmic conduction. At the intermediate voltages (<2.0 kV), the slope of all the samples is less than 2 (inset of Fig. 4). This suggests a trap-free conduction mechanism in these samples. This observation is in agreement with space-charge-limited current conduction,⁴⁰⁻⁴² which is given by

$$J = \frac{9}{8} \varepsilon_r \varepsilon_0 \theta \mu \frac{V^n}{d^3}, \quad (3)$$

where V is the applied field, d is the sample thickness, ε_0 is the permittivity of free space, μ is the mobility, θ is the ratio of free electrons to trapped electrons, and n is the power factor. The estimated value of power factor (n) is about 1.5, 1.3, 1.4, and 1.6 for BiFeO₃, Bi_{0.9}Ca_{0.1}FeO_{2.95}, Bi_{0.9}Ba_{0.05}Ca_{0.05}FeO_{2.95}, and Bi_{0.9}Ba_{0.1}FeO_{2.95}, respectively. At higher voltages (>1.7 kV), the value of power factor (n) increases to ~2 for the undoped and Ca-doped BiFeO₃ samples, in accordance with the steady-state space-charge-limited current conduction mechanism.^{40,42}

Thus, the present study provides an approach for optimizing the electrical and magnetodielectric properties of BiFeO_3 by doping divalent elements, Ca and Ba. Notably, the doped BiFeO_3 materials showed the improved dielectric constant, together with the low dielectric loss and leakage current, as compared to BiFeO_3 . In addition, the Ca-doped samples also have a weak ferromagnetic ordering (induced by chemical pressure) and the enhanced ferroelectric property.³³ These findings make the Ca-doped BiFeO_3 compounds as attractive materials for the ME coupling studies, especially Ca-Ba co-doped sample.

4. SUMMARY

We investigated the electrical and magnetodielectric properties of the BiFeO_3 , $\text{Bi}_{0.9}\text{Ca}_{0.1}\text{FeO}_{2.95}$, $\text{Bi}_{0.9}\text{Ba}_{0.05}\text{Ca}_{0.05}\text{FeO}_{2.95}$, and $\text{Bi}_{0.9}\text{Ba}_{0.1}\text{FeO}_{2.95}$ ceramic materials to compare their material properties. An enhancement in dielectric constant over the wide temperature range is observed by the doping Ca and/or Ba into BiFeO_3 . Notably, the dielectric anomaly near 25 K in BiFeO_3 is shifted towards the higher temperatures (>60 K) upon the doping in conjunction with a broadening of the respective dielectric anomaly. In addition, the switchable magnetodielectric effect for the doped BiFeO_3 materials at room temperature is witnessed and is attributed to the improved magnetoelectric (spin-charge) coupling after the doping. Finally, the lowest leakage current is achieved for the Ba-Ca co-doped BiFeO_3 among the studied materials, which makes it as a potential material for magnetoelectric applications.

ACKNOWLEDGMENT

All authors dedicate this manuscript to late Professor Gavin Lawes (Wayne State University, Detroit, MI, USA) for his encouragement and support for this research. M.S.R.R. acknowledges support from the Department of Science and Technology, India for the project (No. SR/CMP-23/2005). R. Naik acknowledges support from the National Science Foundation through DMR-0644823 and DMR-1306449 and from Wayne State University through a Career Development Chair Award for Prof. Gavin Lawes.

REFERENCES

1. Wang J, Neaton JB, Zheng H, Natarajan V, Ogale SB, Liu B, Viehland D, Vaithyanathan V, Schom DG, Waghmare UV, Spaldin NA, Rabe KM, Wuttig M, Ramesh R. Epitaxial BiFeO₃ multiferroic thin film heterostructures. *Science* 2003;299:1719-1722.
2. Eerenstein W, Mathur ND, Scott JF. Multiferroic and magnetoelectric materials. *Nature* 2006;442:759-765.
3. Catalan G, Scott JF. Physics and Applications of Bismuth Ferrite. *Adv. Mater.* 2009;21:2463-2485.
4. Lebeugle D, Colson D, Forget A, Viret M, Bataille AM, Gukasov A. Electric-field-induced spin flip in BiFeO₃ single crystals at room temperature. *Phys. Rev. Lett.* 2008;100:227602.
5. Fischer P, Polomska M, Sosnowska I, Szymanski M. Temperature dependence of the crystal and magnetic structures of BiFeO₃. *J. Phys. C* 1980;13:1931-1940.
6. Ramachandran B, Ramachandra Rao MS. Low temperature magnetocaloric effect in polycrystalline BiFeO₃ ceramics. *Appl. Phys. Lett.* 2009;95:142505.
7. Spaldin NA, Fiebig M. The renaissance of magnetoelectric multiferroics. *Science* 2005;309:391-392.
8. Ramesh R, Spaldin NA. Multiferroics: Progress and prospects in thin films. *Nat. Mater.* 2007;6:21-29.
9. Lottermoser T, Lonkai T, Amann U, Hohlwein D, Ihringer J, Fiebig M. Magnetic phase control by an electric field. *Nature* 2004;430:541-544.

10. Kimura T, Goto T, Shintani H, Ishizaka K, Arima T, Tokura Y. Magnetic control of ferroelectric polarization. *Nature* 2003;426:55-58.
11. Fiebig M. Revival of the magnetoelectric effect. *J. Phys. D: Appl. Phys.* 2005;38:R123-R152.
12. Srinivasan G, Rasmussen ET, Gallegos J, Srinivasan R, Bokhan Yu I, Laletin VM, Magnetolectric bilayer and multilayer structures of magnetostrictive and piezo oxides. *Phys. Rev. B* 2001;64:214408.
13. Wan JG, Wang XW, Wu YJ, Zeng M, Wang Y, Jiang H, Zhou WQ, Wang GH, Liu JM. Magnetolectric CoFe₂O₄-Pb(Zr,Ti)O₃ composite thin films derived by a sol-gel process. *Appl. Phys. Lett.* 2005;86:122501.
14. Park JH, Jang HM, Kim HS, Park CG, Lee SG. Strain-mediated magnetoelectric coupling in BaTiO₃-Co nanocomposite thin films. *Appl. Phys. Lett.* 2008;92:062908.
15. Singh MP, Prellier W, Simon C, Raveau B. Magnetocapacitance effect in perovskite-superlattice based multiferroics. *Appl. Phys. Lett.* 2005;87:022505.
16. Jang HM, Park JH, Ryu S, Shannigrahi SR. Magnetolectric coupling susceptibility from the magnetodielectric effect. *Appl. Phys. Lett.* 2008;93:252904.
17. Manjunath B, Thakuria P, Joy PA. Structural, magnetic, dielectric and magnetodielectric properties of Bi_{1-x}Ca_xFe_{1-x}Mn_xO₃ in the morphotropic phase boundary region. *Mater. Res. Express* 2017;4:016104.
18. Shankar S, Kumar M, Kumar S, Thakur OP, Ghosh AK. Enhanced multiferroics properties and magneto-dielectric effect analysis of La/Co modified BiFeO₃. *J. Alloys Comp.* 2017;694:715-720.
19. Kamba S, Nuzhnyy D, Savinov M, Šebek J, Petzelt J, Prokleška J, Haumont R, Kreisel J. Infrared and terahertz studies of polar phonons and magnetodielectric effect in multiferroic BiFeO₃ ceramics. *Phys. Rev. B* 2007;75:024403.
20. Liu J, Duan Ch, Mei WN, Smith RW, Hardy JR. Dielectric properties and Maxwell-Wagner relaxation of compounds ACu₃Ti₄O₁₂ (A = Ca, Bi_{2/3}, Y_{2/3}, La_{2/3}). *J. Appl. Phys.* 2005 ;98:093703.
21. Mazumder R, Ghosh S, Mondal P, Bhattacharya D, Dasgupta D, Das N, Sen A, Tyagi K, Sivakumar M, T. Takami T, Ikuta H. Particle size dependence of

- magnetization and phase transition near T_N in multiferroic BiFeO_3 . *J. Appl. Phys.* 2006;100:033908.
22. Catalan G, J. F. Scott JF. Magnetoelectrics: Is CdCr_2S_4 a multiferroic relaxor?. *Nature* 2004;448:E4-E5.
 23. Catalan G. Magnetocapacitance without magnetoelectric coupling. *Appl. Phys. Lett.* 2006;88:102902.
 24. Ramachandran B, Dixit A, Naik R, Lawes G, Ramachandra Rao MS. Dielectric relaxation near 25 K in multiferroic BiFeO_3 ceramics. *J. Appl. Phys.* 2011;110:104105.
 25. Tilley R, Scott JF. Frequency dependence of magnetoelectric phenomena in BaMnF_4 . *Phys. Rev. B* 1982;25:3251.
 26. de Sousa R, Moore JE. Optical coupling to spin waves in the cycloidal multiferroic BiFeO_3 . *Phys. Rev. B* 2008;77:012406.
 27. Ramachandran B, Dixit A, Naik R, Lawes G, Ramachandra Rao MS. Dielectric relaxation and magneto-dielectric effect in polycrystalline $\text{Bi}_{0.9}\text{Ca}_{0.1}\text{FeO}_{2.95}$. *Appl. Phys. Lett.* 2012;100:252902.
 28. Ramachandran B, Wu KK, Kuo YK, Ramachandra Rao MS. Phonon thermal transport and phonon-magnon coupling in bulk BiFeO_3 -based systems. *J. Phys. D: Appl. Phys.* 2015;48:115301.
 29. Caspers C, Ganthi VP, Magrez A, de Rijk E, Ansermet JP. Sub-terahertz spectroscopy of magnetic resonance in BiFeO_3 using a vector network analyzer. *Appl. Phys. Lett.* 2016;108:241109.
 30. Hence LL, West JK (eds). Principles of Electronic ceramics, Wiley Interscience, New York, 1990.
 31. Levinson LM (ed.). Electronic Ceramics: Properties, Devices and Applications, Marcel Dekker, New York, 1988.
 32. Kalinin SV, Suchomel MR, Davies PK, Bonnell DA. Potential and impedance imaging of polycrystalline BiFeO_3 ceramics. *J. Am. Ceram. Soc.* 2002;85:3011-3017.

33. Ramachandran B, Dixit A, Naik R, Lawes G, Ramachandra Rao MS. Weak ferromagnetic ordering in Ca doped polycrystalline BiFeO₃. *J. Appl. Phys.* 2012;111:023910.
34. Yang CH, Seidel J, Kim SY, Rossen PB, Yu P, Gajek M, Chu YH, Martin LW, Holcomb MB, He Q, Maksymovych P, Balke N, Kalinin SV, Baddorf AP, Basu SR, Scullin ML, Ramesh R. Electric modulation of conduction in multiferroic Ca-doped BiFeO₃ films. *Nat. Mater.* 2009;8: 485-493.
35. Popov YF, Zvezdin AK, Vorobev GP, Kadmtseva AM, V. Marushov A, Rakov DN. Linear magnetoelectric effect and phase transitions in bismuth ferrite BiFeO₃. *JETP Lett.* 1993;57:69.
36. Tokunaga M, Azuma M, Shimakawa Y. High-field study of multiferroic BiFeO₃. *J. Phys.: Conf. Series* 2010;200:012206.
37. Ederer C, Spaldin NA. Weak ferromagnetism and magnetoelectric coupling in bismuth ferrite. *Phys. Rev. B* 2005;71:060401.
38. Ederer C, Fennie CJ. Electric-field switchable magnetization via the Dzyaloshinskii-Moriya interaction: FeTiO₃ versus BiFeO₃. *J. Phys.: Condens. Matter* 2008;20:434219.
39. Moriya T. Anisotropic superexchange interaction and weak ferromagnetism. *Phys. Rev.* 1960;120:91.
40. Chang ST, Lee JYM. Electrical conduction in high-dielectric-constant (Ba_{0.5},Sr_{0.5})TiO₃ thin films. *Appl. Phys. Lett.* 2002;80:655.
41. Ramachandran B, Dixit A, Naik R, Lawes G, Ramachandra Rao MS. Charge transfer and electronic transitions in polycrystalline BiFeO₃. *Phys. Rev. B* 2010;82:012102.
42. Sze SM, Physics of semiconductor device, Wiley, New York, 1981.

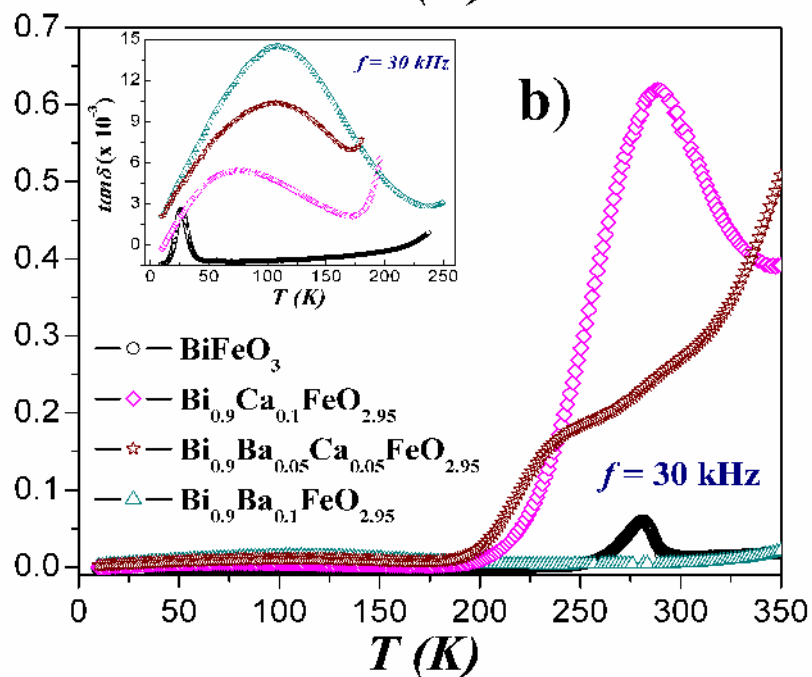
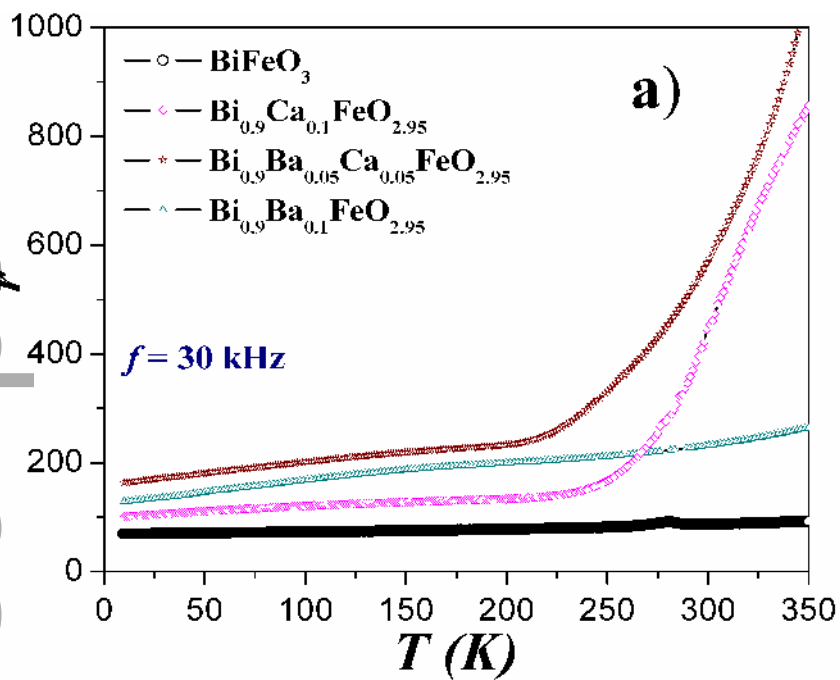
FIGURE CAPTIONS

FIGURE 1 Temperature-dependent a) dielectric constant (ϵ_r) and b) dielectric loss ($\tan\delta$) of the undoped and doped BiFeO₃ samples measured at 30 kHz. Inset of Fig. 1b shows the low-temperature dielectric loss of the samples at 30 kHz.

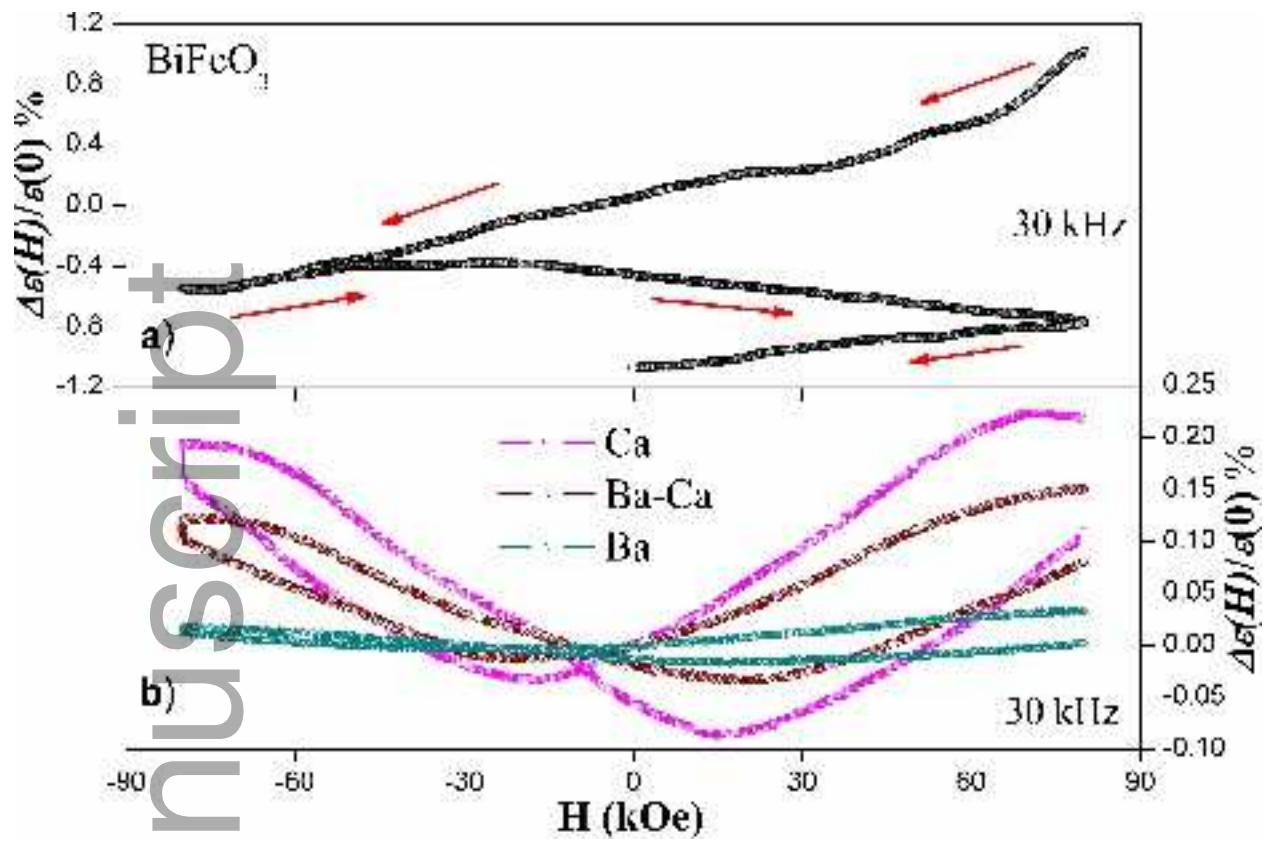
FIGURE 2 Magnetic field dependence of relative dielectric constant of a) undoped and b) doped BiFeO₃ compounds at RT. The arrows in Fig. 2a illustrate the direction of an applied magnetic field.

FIGURE 3 a) The fitted data of $\Delta\epsilon/\epsilon$ vs H at RT for the Ca- and Ba-doped BiFeO₃ samples using the Eq. 2 and b) the plot of $\Delta\epsilon/\epsilon$ vs M for the doped BiFeO₃ samples at RT. Inset of Fig. 3b illustrates the plot of $\Delta\epsilon/\epsilon$ vs M for BiFeO₃.

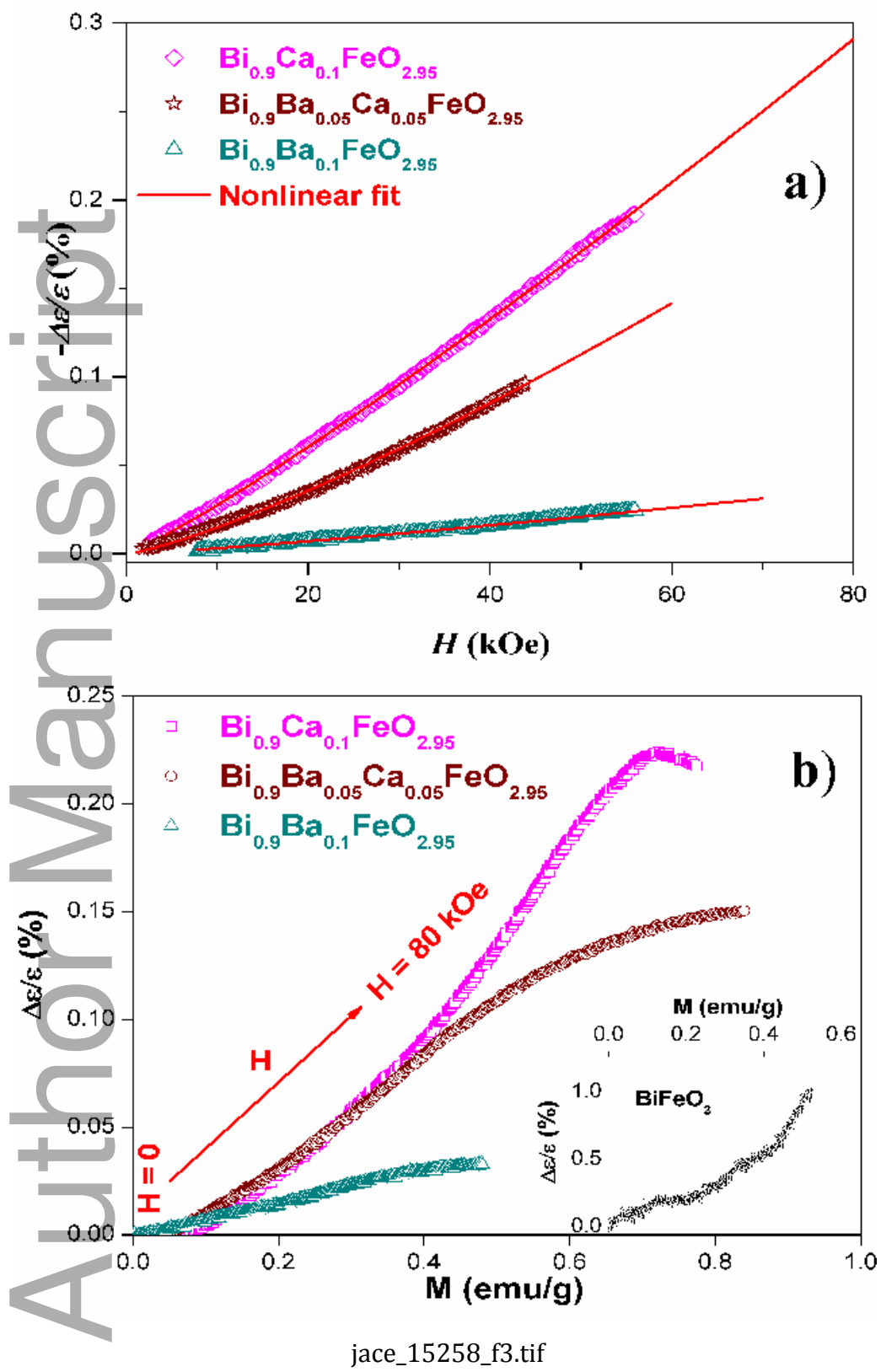
FIGURE 4 Room temperature current density-voltage, J - V (in semi-log scale) characteristics of the undoped and doped BiFeO₃ samples. The inset shows logarithmic plots of J - V of the BiFeO₃-based samples and the solid lines represent the linear fit to the data using the Eq. 3 for the trap-free space-charge conduction mechanism.

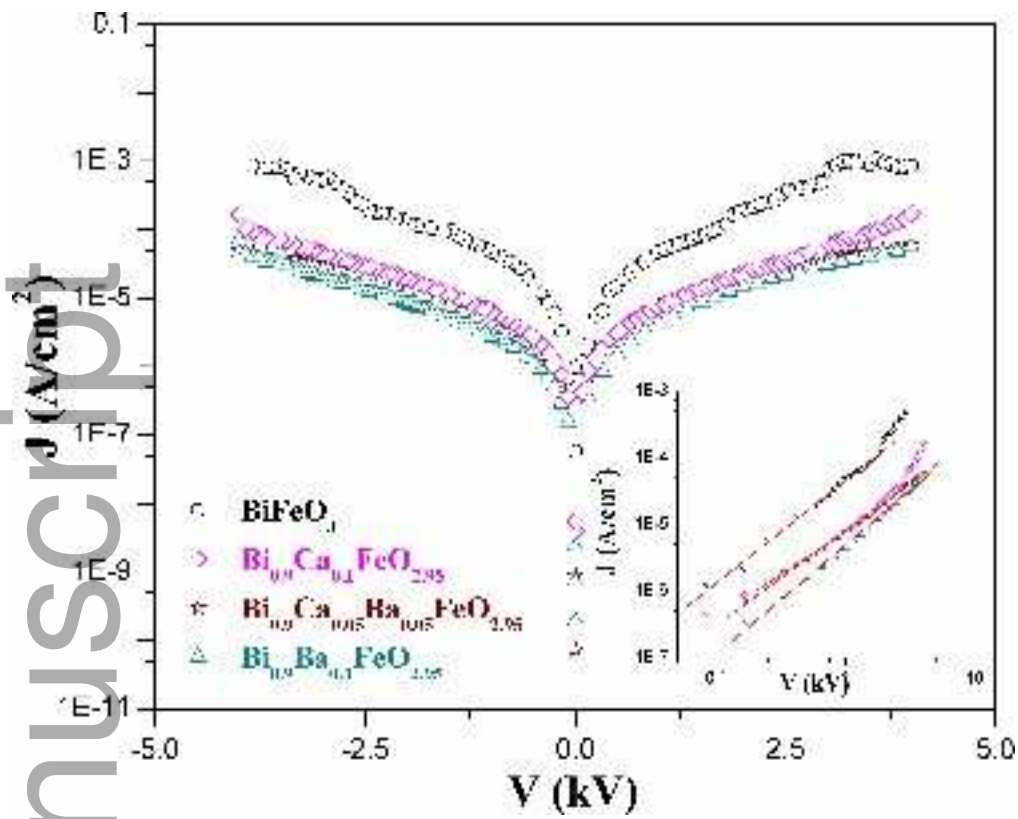


jace_15258_f1.tif



jace_15258_f2.tif





jace_15258_f4.tif